On modelling of shear fracture in deep drawing of a high-strength dual-phase sheet steel

IOP Conf. Series: Journal of Physics: Conf. Series **896** (2017) 012125 doi:10.1088/1742-6596/896/1/012125

On modelling of shear fracture in deep drawing of a high-strength dual-phase sheet steel

B-A Behrens[1], C Bonk[1] and I Peshekhodov[2]

[1] Institute of Forming Technology and Machines (IFUM), Leibniz Universität Hannover, An der Universität 2, 30823 Garbsen, Germany

[2] Advanced Manufacturing Engineering, Faurecia Automotive Seating (FAS), Faurecia S. A., Nordsehler Str. 38, 31655 Stadthagen, Germany

E-mail: ilya.peshekhodov@faurecia.com

Abstract. The paper presents application of fracture behaviour characterisation results of a dual-phase sheet steel DP600 to an FEA of its deep-drawing for shear fracture prediction. The characterisation results were obtained with the help of a characterisation method based on a tensile test on a novel butterfly specimen and published previously by the authors. The aim of the present paper is to evaluate that characterisation method on a deep-drawing process. Based on the previous results of the authors, the fracture behaviour is modelled here with the help of the modified Mohr-Coloumb fracture model. The obtained FEA results reveal that shear fracture of the studied material is predicted too early by the used MMC fracture model. A novel adjustment of the model is proposed yielding infinitely high fracture strains at strongly pressure-superimposed stress states. As it is often the case in the state-of-the-art fracture characterisation of high-strenght sheet steels, such stress states were not tested during the previously performed fracture characterisation but occur during the studied deep drawing process. With the help of the adjusted MMC fracture model, it is possible to predict the crack initiation moment very accurately and the crack initiation location sufficiently accurately.

1. Introduction

To fulfil the legal regulations on carbon dioxide emissions, car manufacturers have been using more light-weight materials. In the harsh material competition, steel materials are expected to loose their traditionally high share over the next years [1]. To slow down the anticipated decrease of steel consumption in the automotive industry, steel manufacturers are forced to work hard on continuous improvement of high-strength sheet steel but also on efficient solutions for a better exploitation of their high potential in car weight reduction at acceptable costs. A better exploitation of this potential requires an accurate modelling of the material behaviour under loading conditions of forming and crash, in particular yielding, hardening and formability.

Traditionally, forming limit curves (FLC) have been used to describe formability of a sheet metal [2]. However, crack initiation at the transition area between the flange and the skirt of a high-strength steel workpiece in a deep drawing process cannot be predicted with the FLC. This type of failure occurs mainly due to plastic deformation in the flange, which takes place under a shear-dominated stress state. The standardised procedure for the FLC determination [3] does not imply material testing at such a stress state, which consequently makes it inappropriate to predict shear fracture. Especially dual-phase steels are prone to such failure due to their microstructure consisting of two mechanically dissimilar phases [4].

To predict crack initiation due to plastic deformation under a shear-dominated stress state, fracture initiation models, which on an incremental basis consider both the accumulated plastic strain and the stress state, at which this plastic deformation takes place, can be used [5]. Most of these models predict fracture initiation, which occurs without a noteworthy plastic strain localisation at a shear-dominated stress state, with the help of an accumulated equivalent plastic strain $\bar{\varepsilon}_{\mathrm{pl}}$, which is weighted with a function of the stress state $f(\sigma)$ and compared with a material-specific stress-state-dependent fracture strain $\bar{\varepsilon}^{\mathrm{f}}_{\mathrm{pl}}$.

There exist many mathematical formulations to describe the material formability depletion rate with plastic deformation depending on the stress state [6, 7]. To quantify a three-dimensional stress state for this purpose, the stress triaxiality η and the normalised Lode angle $\bar{\theta}$ have become frequently used [8, 9]. The stress triaxiality η is defined by:

$$\eta = \frac{\sigma_{\mathrm{m}}}{\bar{\sigma}} \in (-\infty; +\infty)\,, \tag{1}$$

where σ_{m} is the mean major stress and $\bar{\sigma}$ is the equivalent stress. The normalised Lode angle $\bar{\theta}$:

$$\bar{\theta} = 1 - \frac{2}{\pi}\arccos\xi \in [-1; 1]\,, \tag{2}$$

is defined via the parameter of the Lode angle ξ given by:

$$\xi = \frac{27\,(\sigma_{\mathrm{I}} - \sigma_{\mathrm{m}})\,(\sigma_{\mathrm{II}} - \sigma_{\mathrm{m}})\,(\sigma_{\mathrm{III}} - \sigma_{\mathrm{m}})}{2\left(1/2\left[(\sigma_{\mathrm{I}} - \sigma_{\mathrm{II}})^2 + (\sigma_{\mathrm{II}} - \sigma_{\mathrm{III}})^2 + (\sigma_{\mathrm{I}} - \sigma_{\mathrm{III}})^2\right]\right)^{3/2}} \in [-1; 1]\,, \tag{3}$$

where σ_{I}, σ_{II} and σ_{III} are the major stresses. For two-dimensional stress states, which are often assumed in sheet metal forming, there exist a functional relation between the stress triaxiality η and normalised Lode angle $\bar{\theta}$. As a result, the stress triaxiality η is sufficient for their description [8, 9]. In this case, $\eta = 0$ represents plane shear, $\eta = 0.33$ corresponds to uniaxial tension, $\eta = 0.58$ describes plane strain and $\eta = 0.67$ gives equibiaxial tension.

To predict crack initiation due to shear band localisation in a high-strength sheet, CrachFEM shear fracture model [10] or modified Mohr-Coloumb (MMC) fracture model [11] can be used used [12, 13]. It was shown that the MMC fracture model gives more flexibility in approximation of fracture strains and can thus yield a more accurate description of the fracture behaviour of a high-strength dual-phase sheet steel DP600 [14]. The fracture strain $\bar{\varepsilon}^{\mathrm{f}}_{\mathrm{pl}}$ is given by this model as follows:

$$\begin{aligned}\bar{\varepsilon}^{\mathrm{f}}_{\mathrm{pl}} = \Bigg\{ \frac{A}{C_2}\Bigg[C_3 + \frac{\sqrt{3}}{2-\sqrt{3}}\,(1 - C_3)\left(\sec\left(\frac{\bar{\theta}\pi}{6}\right) - 1\right)\Bigg] \\ \times \Bigg[\frac{\sqrt{1 + C_1^2}}{3}\cos\left(\frac{\bar{\theta}\pi}{6}\right) + C_1\left(\eta + \frac{1}{3}\sin\left(\frac{\bar{\theta}\pi}{6}\right)\right)\Bigg]\Bigg\}^{-1/n},\end{aligned} \tag{4}$$

where A/C_2, C_1, C_3 and n are model parameters.

The damage variable D, which can be considered as a degree of formability depletion, is:

$$D = \sum_i \frac{\Delta\bar{\varepsilon}_{\mathrm{pl}i}}{\bar{\varepsilon}^{\mathrm{f}}_{\mathrm{pl}}} \in [0; 1]\,, \tag{5}$$

where $\bar{\varepsilon}_{\mathrm{pl}i}$ is the equivalent plastic strain of the simulation increment i.

The aim of the present paper is to evaluate the fracture characterisation method based on a tensile test on a novel butterfly specimen, which was proposed by the authors in a previous publication [14], on an FEA of a deep-drawing process of a dual-phase high-strength sheet steel DP600. In case of considerable discrepancies between the experiment and simulation with respect to the time moment and location of shear fracture initiation, novel improvements of the characterisation method or the used fracture modelling approach are to be proposed.

2. Experimental set-up

The used forming tool consists of a punch and a die, which have a rectangular cross-section, as well as a flat blank holder. The dimensions of the punch and the die are presented in figure 1. The geometry of the used blank with a thickness of 1.4 mm can be seen in figure 2, right. The geometry of the tools and the blank was chosen based on the motivation to induce crack initiation in the workpiece at the transition area between the flange and the skirt at the die edge radius. The crack initiation in this area occurs mainly due to plastic deformation in the flange under a shear-dominated stress state. The crucial role for the crack initiation in this area is played by the ratio between the radius of the punch edge of 6 mm and radius of the die edge of 3 mm, which helped avoid strain localisation at the corner of the punch. Similar tool geometry principles were already used by other authors to induce shear fracture in a high-strenght steel sheet [13].

The tool was set up in the hydraulic press HDPZb 63 of IFUM with the maximum punch force of 630 kN and maximum blank holder force of 400 kN. The tool set-up in the press can be seen in figure 2, left. To minimise the influence of friction on the result of the deep-drawing process, a deep-drawing polymer foil and lubricant Raziol CLF 200 of Zibulla & Sohn GmbH were applied to both sides of the blanks. The blank holder force was maintained constant at 320 kN during the whole process to suppress folds in the flange. The punch velocity was kept equal to 10 mm/s to ensure both an adequate duration of the experiments and a quasistatic workpiece deformation. Four cups were formed up to the cup depth of 23 mm, 24 mm and 25 mm each.

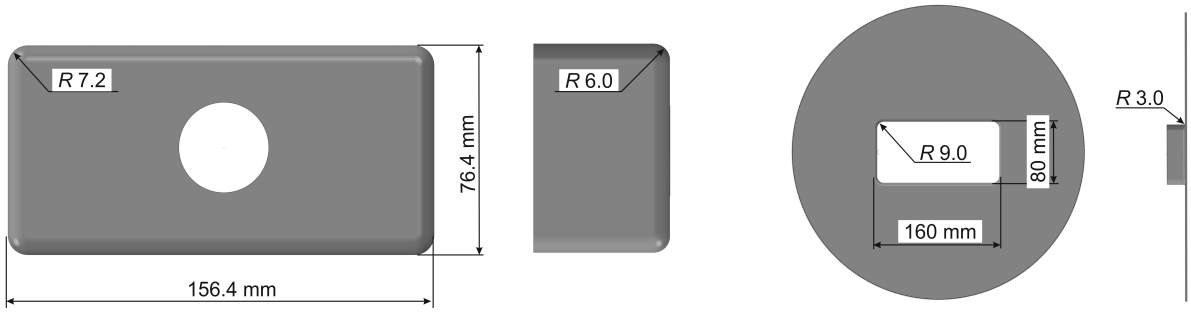

Figure 1. Geometry of the punch (left) and die (right).

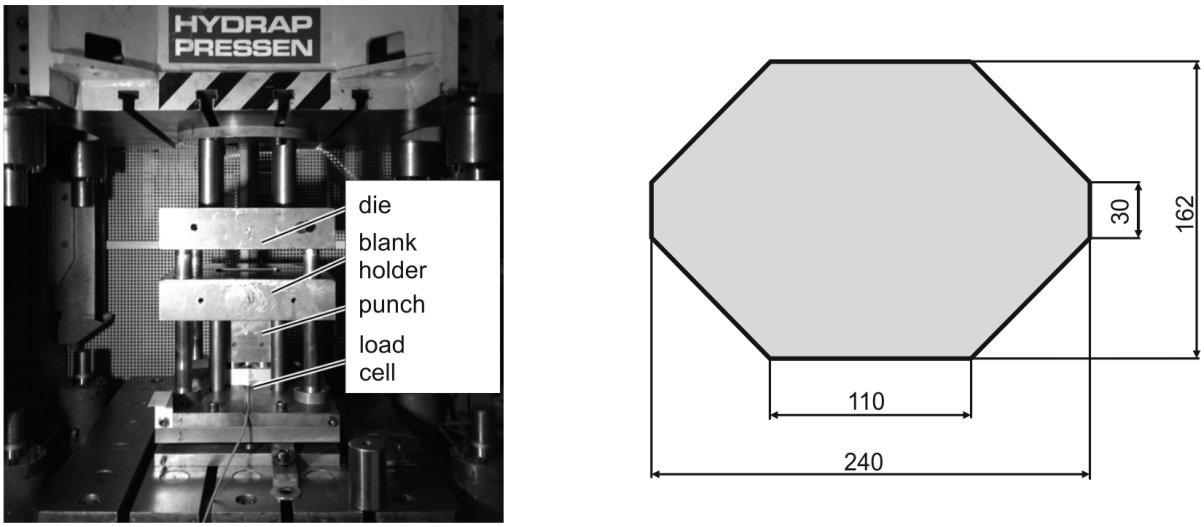

Figure 2. Tool set-up in the press (left) and geometry of the blank (right).

3. Simulation set-up

The deep-drawing experiments were simulated with the help of a finite element model realised in Abaqus/Explicit. The tool components were modelled ideally rigid. An elasto-plastic material model with the Hill'48 yield condition ($F = 0.460$, $G = 0.534$, $H = 0.466$, $N = 1.366$, $L = 1.5$ and $M = 1.5$) and isotropic hardening approximated by the Swift-Hocket-Sherby law given by:

$$\bar{\sigma} = 0.479 \cdot \left(642 \cdot (0.00596 + \bar{\varepsilon}_{\mathrm{pl}})^{0.660}\right) + 0.521 \cdot \left(1224 - (1224 - 757) \cdot e^{-15.5 \cdot \bar{\varepsilon}_{\mathrm{pl}}^{0.820}}\right) \quad (6)$$

was assigned to the workpiece (figure 3). The fracture behaviour was described by the MMC fracture model according to equation 4 with $A/C_2 = 1.667$, $n = 0.635$, $C_1 = 0.291$,$C_3 = 1.070$ as proposed in [14] for a virtual strain gauge length of $l_0 = 0.2\,\mathrm{mm}$. Furthermore, following results of Bao and Wierzbicki [15], who pointed out at a cut-off value of the stress triaxiality of $\eta = -0.33$, below which fracture in a steel material never occurs, the fracture behaviour was also described by an adjusted MMC fracture model, which yields infinitely high fracture strains $\bar{\varepsilon}_{\mathrm{pl}}^{\mathrm{f}}$ at stress triaxialities of $\eta \leq -0.33$ as shown in figure 4, right. Both fracture behaviour descriptions were implemented in Abaqus/Explicit in the form of data sets $[\eta; \xi; \bar{\varepsilon}_{\mathrm{pl}}^{\mathrm{f}}]$. The workpiece was discretised with linear solid elements of reduced integration with an hour-glass control C3D8R with an element size of around 0.4 mm. The friction coefficient was set to be $\mu = 0.04$.

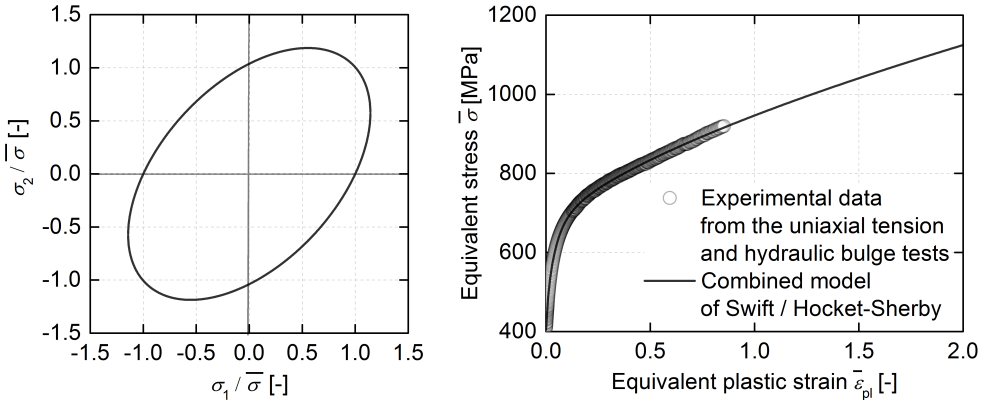

Figure 3. Hill'48 yield condition (left) and flow curve (right) of the studied material DP600.

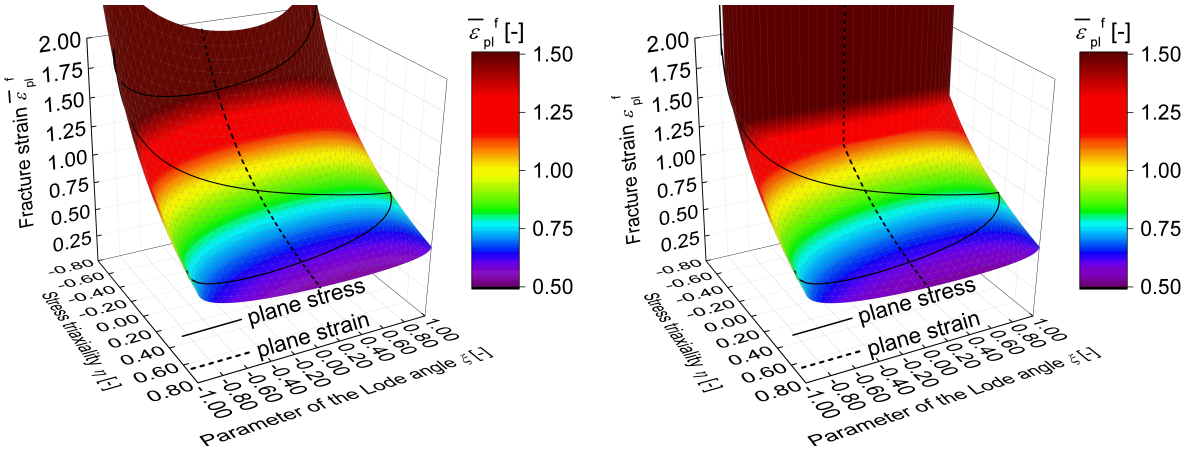

Figure 4. MMC (left) and adjusted MMC fracture model (right) of the studied material DP600.

4. Results and discussion

A validation of the mathematical description of the workpiece flow behaviour and friction between the workpiece and tool was performed based on a comparison of cup geometry parameters and punch forces from the experiment and simulation for the cup depth of 24 mm. At this cup depth, 50 % of the parts exhibit a small crack at the transition area between the flange and skirt. All parts drawn up to the depth of 23 mm were free of cracks, whereas a crack was detected in all parts drawn up to the depth of 25 mm. Results of the cup geometry parameters comparison are shown in figure 5 and reveal a good agreement between the experiment and simulation. The higher experimental cup depth is explained with a light curvature of the cup bottom, which occured upon removal of the part from the tool. The removal of the part from the tool was not numerically simulated as the experimental springback was found negligible. The punch forces (figure 6, left) coincide well, especially at their maximum values. The noteworthy deviation between the experimental and numerical punch forces takes place only towards the end of the process. This deviation can be primarily explained with an assumption of the contact-pressure-independent friction coefficient $\mu = 0.04$ in the model, which in reality is expected to be lower at higher contact pressures between the workpiece and tool. Alternatively, even though to a lesser degree, it can be explained with accumulated damage in the workpiece at high plastic strains, which reduces its resistance to plastic deformation and was not considered in the model.

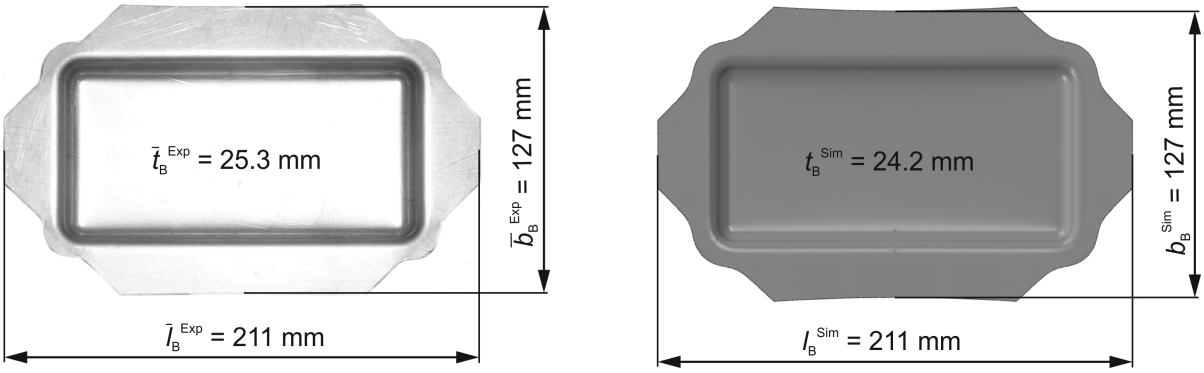

Figure 5. Experimentally (left) and numerically (right) determined part geometry.

Figure 6, left also shows the fulfilment of the condition $D \geq 1$ for the outer radius, middle plane and inner radius of the workpiece at the die edge radius (s. also figure 7). In figure 6, right, the development of the damage variable D for these material points depending on the punch displacement u_{St} is shown. It can be seen that the increase of the damage variable D is the fastest at the outer radius and the slowest at the inner radius, which is attributed to workpiece bending. Accordingly, crack initiation is expected to occur at the outer radius first and then at the inner radius. Independent of the workpiece fracture definition (right after the fulfilment of the condition $D \geq 1$ at the outer radius or only after the fulfilment of this condition through the whole sheet thickness), the used MMC fracture model predicts crack initiation too early.

The development of the stress triaxiality η in the critical finite elements at the outer radius, middle plane and inner radius at the die edge radius, in which the condition $D \geq 1$ is first fulfilled is shown in figure 11, left. As can be seen, the critical element at the inner radius experiences a strongly pressure-superimposed stress state with stress triaxialities η below -0.33. Taking into consideration the fact that fracture strains of the studied material used for the parameterisation of the MMC fracture model were determined at stress triaxialites of $\eta \geq 0$ [14] and findings of Bao and Wierzbicki [15] who postulated no damage accumulation in metallic materials at stress triaxialities of $\eta \leq -0.33$, the MMC fracture model was adjusted to yield infinitely high fracture strains $\bar{\varepsilon}_{pl}^{f} = +\infty$ at $\eta \leq -0.33$ (compare figure 4, left and right).

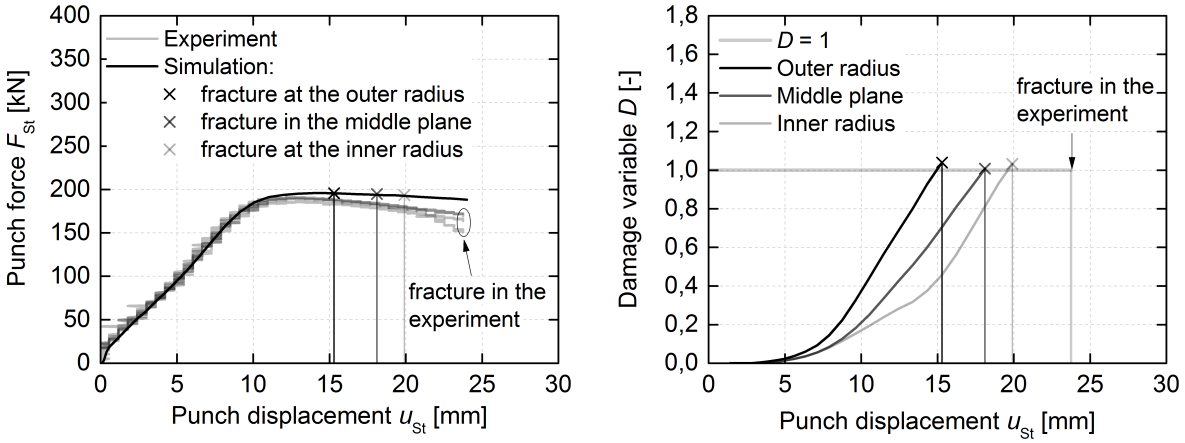

Figure 6. Experimentally and numerically determined punch forces F_{St} (left) and damage variable D according to the MMC fracture model for different critical elements (right).

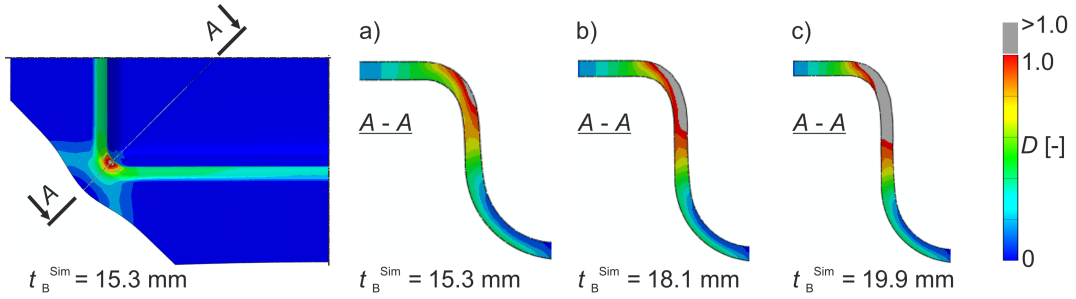

Figure 7. Damage variable D according to the MMC fracture model in the deep-drawn cup at different cup depths $t_{\mathrm{B}}^{\mathrm{Sim}}$ with $D \geq 1$ at the outer radius (a), at the outer radius and middle plane (b) and through the entire sheet thickness (c).

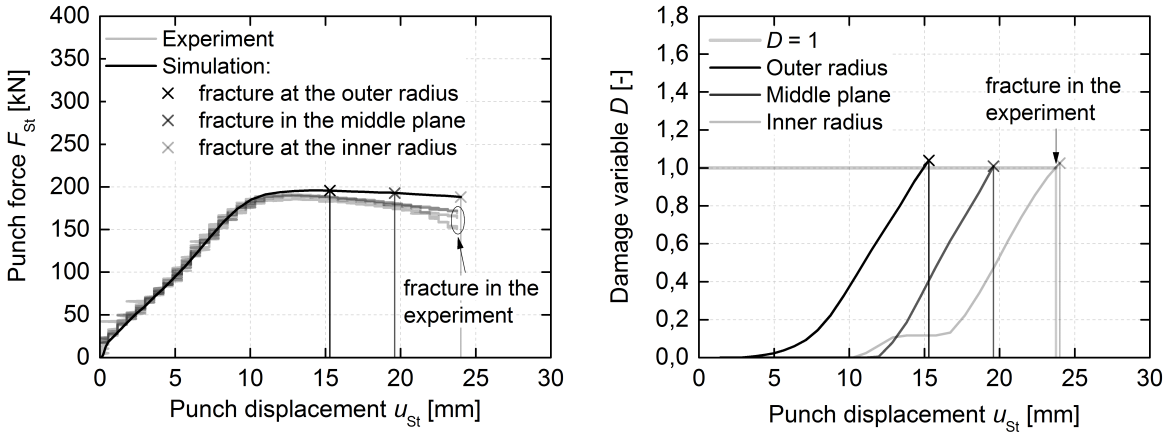

Figure 8. Experimentally and numerically determined punch forces F_{St} (left) and damage variable D according to the adjusted MMC fracture model for different critical elements (right).

The adjustment of the MMC fracture model lead, as expected, to a delay in crack initiation in critical elements in the middle plane and at the inner radius, as can be seen in figure 8 and figure 9. With the adjusted MMC fracture model, the condition $D \geq 1$ is fulfilled in the middle plane at the cup depth of $t_B^{Sim} = 19.6\,mm$ instead of $t_B^{Sim} = 18.1\,mm$ and at the inner radius at the cup depth of $t_B^{Sim} = 24.0\,mm$ instead of $t_B^{Sim} = 19.9\,mm$ (compare figure 9 and figure 7). With an assumption that macroscopic fracture of the workpiece in the simulation occurs only upon the fulfilment of the condition $D \geq 1$ through the whole sheet thickness, the process simulation with the adjusted MMC model predicts the cup depth t_B^{Sim}, at which workpiece fractures, with a good accuracy. The position of the crack initiation in the simulation is determined with a sufficient accuracy as can be seen in figure 10. Figure 10, left reveals that the crack in the real part initiates in the transition area between the radius at the die edge radius and the straight skirt and extends along the areas of high shear deformation into the flange. This result goes well in accordance with findings of the research project "ENFASS", in which formability of high-strength sheet steels at stretch-bending was investigated [16]. According to the project findings, crack initiation in a high-strength sheet steel is delayed during stretch-bending and takes place with a high probability at the moment when the sheet leaves the radius, over which it has been stretch-bent, and is bent straight [16]. If the workpiece fracture – as assumed in the present paper – occurs only upon the fulfilment of the condition $D \geq 1$ through the whole sheet thickness, the performed process simulation predicts failure not exactly at the position where the workpiece is bent straight, but at a small offset into the skirt as figure 9 or figure 10, right show. This accuracy in the prediction of the crack initiation position is considered sufficient.

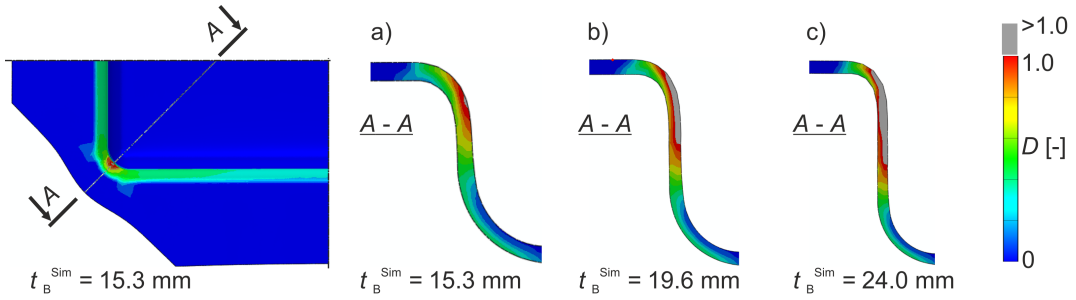

Figure 9. Damage variable D according to the adjusted MMC fracture model in the deep-drawn cup at different cup depths t_B^{Sim} with $D \geq 1$ at the outer radius (a), at the outer radius and middle plane (b) and through the entire sheet thickness (c).

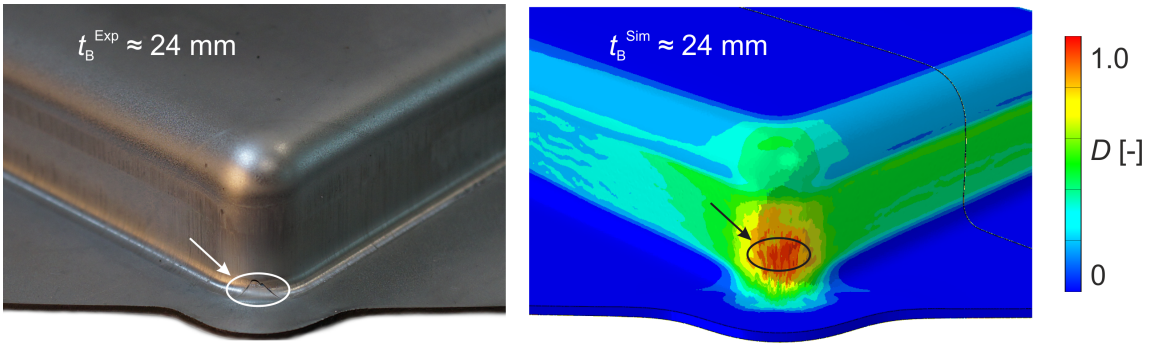

Figure 10. Position of the crack in the real part (left) and in the virtual part obtained with the help of the adjusted Mohr-Coloumb fracture model (right).

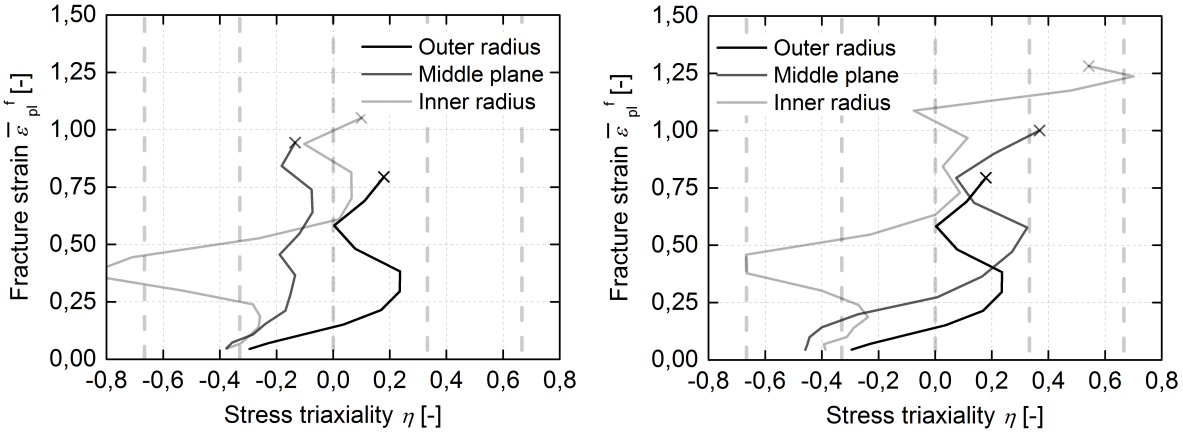

Figure 11. Development of the stress state in different critical elements of the workpiece according to the MMC fracture model (left) and adjusted MMC fracture model (right).

5. Conclusion and outlook

An evaluation of the fracture characterisation method based on a tensile test on a novel butterfly specimen, which was previously proposed by the authors [14], on an FEA of a deep-drawing process of a dual-phase sheet steel DP600 is presented. The results reveal that shear fracture of this material is predicted too early by the used MMC fracture model. A novel model adjustment is proposed with infinitely high fracture strains at strongly pressure-superimposed stress states. With the help of the adjusted MMC fracture model, it is possible to predict the crack initiation moment very accurately and the crack initiation location sufficiently accurately.

Acknowledgements

A part of the findings was gained in the frame of the project P 972 of the Research Association for Steel Application (FOSTA), Dusseldorf, Germany, funded by the German Federation of Industrial Research Associations (AiF). The financial support of AiF, project coordiation of FOSTA and technical support of the industrial project committee are gratefully acknowledged.

References

[1] Heuss R, Müller N, van Sintern W, Starke A and Tschiesner A 2012 *Lightweigt, heavy impact. Advanced industries report.* (McKinsey & Company)
[2] Banabic D 2010 *Sheet metal forming processes. Constitutive modelling and numerical simulation* (Springer)
[3] 2006 *ISO 12004-2 Metallic materials – Sheet and strip – Determination of formig limit curves – Part 2* (ISO)
[4] Sun X, Choi K S, Liu W N and Khaleel M A 2009 *International Journal of Plasticity* **25** 1888
[5] Atkins A G 1996 *Journals of Materials Processing Technology* **56** 609
[6] Bao Y and Wierzbicki T 2004 *Transactions of the ASME* **126** 314
[7] Wierzbicki T, Bao Y, Lee Y-W and Bai Y 2005 *International Journal of Mechanical Sciences* **47** 719
[8] Till E and Hackl B 2013 *Proc. of the IDDRG Conf.* (IVP, ETH Zurich)
[9] Wierzbicki T and Bai Y 2013 *Proc. of the IDDRG Conf.* (IVP, ETH Zurich)
[10] Dell H, Gese H and Oberhofer G 2007 *Proc. of the NUMIFORM Conf. in AIP Conf. Proc.* **908** 165
[11] Beese A M, Luo M, Li Y, Bai Y and Wierzbicki T 2010 *Engineering Fracture Mechanics* **77** 1128
[12] Isik K, Soyarslan C, Richter H and Tekkaya A E 2011 *Proc. of the Europ. LS-Dyna Conf.* (Dynamore) 1
[13] Li Y, Luo M, Gerlach J and Wierzbicki T 2010 *Journal of Materials Processing Technology* **161** 1858
[14] Peshekhodov I, Jiang S, Vucetic M, Bouguecha A and Behrens B-A 2016 *Proc. of the IDDRG Conf. in IOP Conf. Series: Materials Science and Engineering* **159** 012015
[15] Bao Y and Wierzbicki T 2005 *Engineering Fracture Mechanics* **7** 1049
[16] Weiß W, van den Boogard T, Till E, Atzema E and Grünbaum M 2014 *Enhanced Formability Assessment of AHSS Sheets. Project report* (Research Fund for Coal and Steel, European Comission)